

Information Maximization via Variational Autoencoders for Cross-Domain Recommendation

Xuying Ning[†]
Xi'an Jiaotong University
Xi'an, China

Xiaolei Liu, Mingming Ha, Qiong Xu Ma
Youru Li, Linxun Chen
MYbank, Ant Group
Hangzhou, China

Wujiang Xu[†]
Rutgers University
New Brunswick, US

Yongfeng Zhang*
Rutgers University
New Brunswick, US

ABSTRACT

Cross-Domain Sequential Recommendation (CDSR) methods aim to address the data sparsity and cold-start problems present in Single-Domain Sequential Recommendation (SDSR). Existing CDSR methods typically rely on overlapping users, designing complex cross-domain modules to capture users' latent interests that can propagate across different domains. However, their propagated informative information is limited to the overlapping users and the users who have rich historical behavior records. As a result, these methods often underperform in real-world scenarios, where most users are non-overlapping (cold-start) and long-tailed. In this research, we introduce a new CDSR framework named Information Maximization Variational Autoencoder (**IM-VAE**). Here, we suggest using a Pseudo-Sequence Generator to enhance the user's interaction history input for downstream fine-grained CDSR models to alleviate the cold-start issues. We also propose a Generative Recommendation Framework combined with three regularizers inspired by the mutual information maximization (MIM) theory [23] to capture the semantic differences between a user's interests shared across domains and those specific to certain domains, as well as address the informational gap between a user's actual interaction sequences and the pseudo-sequences generated. To the best of our knowledge, this paper is the first CDSR work that considers the information disentanglement and denoising of pseudo-sequences in the open-world recommendation scenario. Empirical experiments illustrate that IM-VAE outperforms the state-of-the-art approaches on two real-world cross-domain datasets on all sorts of users, including cold-start and tailed users, demonstrating the effectiveness of IM-VAE in open-world recommendation.

CCS CONCEPTS

• **Information systems** → **Recommender systems**; • **Computing methodologies** → **Neural networks**.

KEYWORDS

Cross-Domain Sequential Recommendation, Sequential Recommendation, Mutual Information Maximization, Variational Autoencoder

*Corresponding author.

[†] Joint first author.

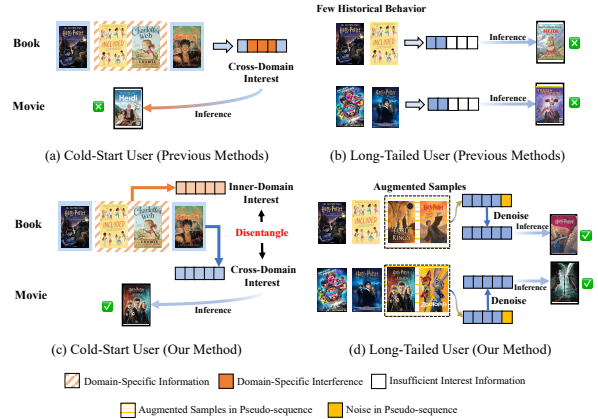


Figure 1: Previous methods [2, 15, 21] transfer cross-domain information that is not disentangled and insufficiently capture the interests of long-tailed users, losing the performance to the cold-start and long-tailed users. IM-VAE learns the disentangled cross-domain and inner-domain interests and utilizes the denoised information to enhance the performance for cold-start and long-tailed users.

1 INTRODUCTION

With the rise of various sequential models, single-domain sequential recommendation (SDSR) [8, 12, 29, 31, 32] has gained increased attention due to its ability to model users' dynamic interests in recommendation systems. However, these SDSR models often suffer from the long-standing data sparsity problem [17, 35], where new users have no prior interactions in a domain to learn their preferences effectively. To address this issue, cross-domain sequential recommendation (CDSR) methods [2, 15, 20, 21] have been proposed to leverage rich information from other relevant domains to improve recommendation performance in a sparser domain.

The core idea of CDSR is to extend SDSR methods by designing cross-domain information transfer modules to capture domain-shared interests that can be transferred across domains. Researchers have employed various techniques, including gating mechanisms [21, 30], attention mechanisms [15, 36], graph neural networks [6, 20], and contrastive learning [2, 36], to learn user interests that can be transferred across domains. These learned cross-domain interests are then used to supplement the interest representations of overlapping users (users who appear in each domain) and to infer the cross-domain interests for cold-start users¹.

¹Cold-start users are those with interaction records in one domain and none in another.

Although it appears promising, we find that previous CDSR methods [2, 15, 21, 22] heavily rely on overlapping users with rich historical behaviors. They can only effectively learn users' cross-domain interests when a majority (over 70%, as noted by [37]) of users are overlapping across domains, and only adequately capture intra-domain interests when users have extensive historical interactions. However, these conditions are rarely met in real-world recommendation tasks [36, 37], where the majority of users are cold-start or long-tailed²). For instance, on platforms like Taobao or Amazon, there are very few overlapping users compared to the entire user base (including overlapping and non-overlapping users), and most users have very few interaction records (a.k.a. long-tailed users). In such cases, these CDSR methods, trained on the sparse historical behaviors of a few overlapping users, often show poor generalization, especially when inferring the intra-domain and cross-domain interests of cold-start and long-tailed users. This presents the **primary challenge**: how to enhance the CDSR model's performance in real-world recommendation scenarios, where most users are either cold-start or long-tailed?

Suffering from cold-start users, previous CDSR and CDR works have often utilized cross-domain modules that learn a mapping function from one domain to another based on the historical behaviors of overlapping users [11, 27, 28, 39]. However, the absence of historical behavior data for cold-start users hinders previous methods from effectively transferring cross-domain information. For example, as depicted in Figure 1(a), prior techniques transfer domain-specific interest information from the book domain, which may be irrelevant or even detrimental to the movie domain and could potentially deteriorate, rather than enhance, the model's performance. Therefore, the **1st sub-challenge** is: *How to transfer relevant cross-domain information for cold-start users who lack historical interest data?* Meanwhile, to address insufficient interest learning of the predominant presence of long-tailed users in real-world scenarios (Figure 1(b)) and to enhance model performance, MACD [36] employs attention mechanisms to discern latent interests from auxiliary sequential behavior data. However, such auxiliary behaviors may not always be available. Therefore, the **2nd sub-challenge** is: *How to unearth and leverage the latent interest information of long-tailed users, thereby improving model performance in practical cross-domain sequential recommendation (CDSR) scenarios?*

To this end, we propose an Information Maximization Variational Autoencoder, named IM-VAE, to tackle these challenges. It includes a pseudo-sequence generator, VAEs, and three novel informational regularizers (informative, disentangle, and denoising) induced by the mutual information maximization theory[5, 23]. IM-VAE effectively explores the latent interest information of long-tailed users and transfer disentangled cross-domain interest information for overlapping users and cold-start users, which significantly improve the model's performance in real-world scenarios. As a summary, our main contributions can be highlighted as follows:

- A information maximization variational autoencoder (IM-VAE) is proposed towards real-world CDSR scenarios. Different from previous methods, it considers extracting interest information for the cold-start users and long-tailed users.

- To enhance the model's robustness cold-start users in partially overlapped CDSR scenarios, we propose a novel MIM theory-induced information and disentangle regularizers by facilitating the joint learning and separation of users' intra- and cross-domain interests.
- To improve the model's performance for long-tailed users, we propose a pseudo-sequence generator combined with a denoising regularizer that augments user interaction behaviors and effectively eliminates noise pseudo-sequences.
- We demonstrate that the proposed IM-VAE attains SOTA performance when benchmarked against SDSR, CDR, and CDSR in real-world cross-domain scenarios. Uniquely, the IM-VAE systematically quantifies the enhancement for long-tailed and cold-start users across all experiments, distinguishing it from prior methods.

2 PRELIMINARY

2.1 Problem Formulation

In this work, we consider a general Cross-Domain Sequential Recommendation (CDSR) scenario that includes a part of overlapping users, and a majority of long-tailed and cold-start users across two domains, namely domain X and domain Y . The interaction data is represented by $D^X = (U^X, V^X, \mathcal{E}^X)$ and $D^Y = (U^Y, V^Y, \mathcal{E}^Y)$, where U , V , and \mathcal{E} are the sets of users, items, and interaction edges, respectively. For a given user, we denote their item interaction sequences in chronological order as $S^X = [v_1^X, v_2^X, \dots, v_{|S^X|}^X]$ and $S^Y = [v_1^Y, v_2^Y, \dots, v_{|S^Y|}^Y]$, where $|\cdot|$ denotes the length of the sequence. The objective of CDSR is to predict the next item for a given user based on the user's behavior sequence in both domains:

$$\begin{aligned} & \operatorname{argmax}_{v_i \in V^X} P^X(v_i | S^X, S^Y), \text{ if next item } \in V^X, \\ & \operatorname{argmax}_{v_i \in V^Y} P^Y(v_i | S^X, S^Y), \text{ if next item } \in V^Y. \end{aligned}$$

2.2 Mutual Information

An important technique in our approach is Mutual Information Maximization (MIM) [1, 9, 23], based on the concept of mutual information[10, 24]. For two random variables \mathcal{X} and \mathcal{Y} , mutual information quantifies how much knowing \mathcal{X} reduces uncertainty in \mathcal{Y} , and vice versa. Formally, it is defined as:

$$I(\mathcal{X}; \mathcal{Y}) = H(\mathcal{X}) - H(\mathcal{X} | \mathcal{Y}) = H(\mathcal{Y}) - H(\mathcal{Y} | \mathcal{X}) = I(\mathcal{Y}; \mathcal{X}), \quad (1)$$

where $H(\mathcal{X})$ and $H(\mathcal{Y})$ represent the entropy of \mathcal{X} and \mathcal{Y} , and $H(\mathcal{X} | \mathcal{Y})$ and $H(\mathcal{Y} | \mathcal{X})$ represent the conditional entropy of \mathcal{X} given \mathcal{Y} , and \mathcal{Y} given \mathcal{X} , respectively.

Moreover, interaction information[23] quantifies the amount of information shared among three variables that is not captured by pairwise mutual information alone. The interaction information between \mathcal{X} , \mathcal{Y} , and \mathcal{Z} is defined as:

$$I(\mathcal{X}; \mathcal{Y}; \mathcal{Z}) = I(\mathcal{X}; \mathcal{Y}) - I(\mathcal{X}; \mathcal{Y} | \mathcal{Z}) \quad (2)$$

$$= I(\mathcal{X}; \mathcal{Z}) - I(\mathcal{X}; \mathcal{Z} | \mathcal{Y}) \quad (3)$$

$$= I(\mathcal{Y}; \mathcal{Z}) - I(\mathcal{Y}; \mathcal{Z} | \mathcal{X}) \quad (4)$$

3 METHODOLOGY

In this section, we will introduce the pseudo-sequence generator, the inference and generation procedures of IM-VAE, and three information regularizers (informative, disentangle, and denoising) designed in our model. Figure 2 provides an overview of IM-VAE.

²Long-tailed users are those with a few interaction records.

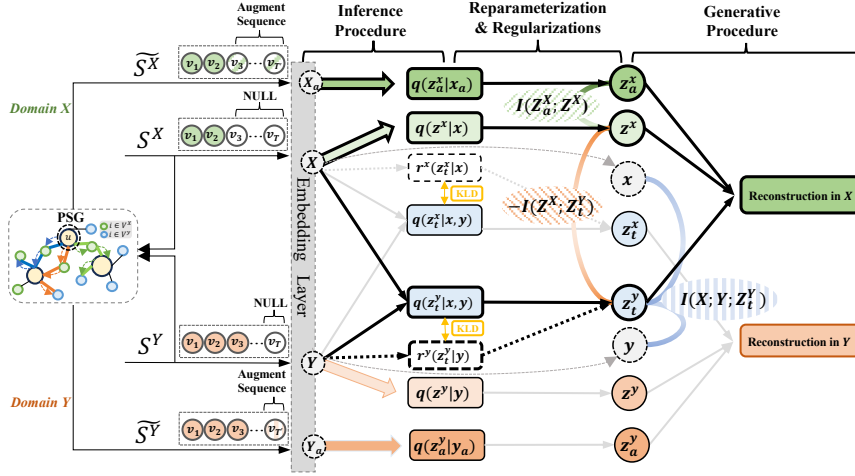


Figure 2: Overview of our IM-VAE approach. We primarily highlight the computational pathways (black lines) and the design of regularization terms (colored striped backgrounds) for predictions in the domain X , with a fully symmetric design for the domain Y . The dashed-line component $r^y(z_t^y|y)$ is used in place of the cross-domain module $q(z_t^y|x, y)$ when faced with cold-start users in domain X .

3.1 Pseudo-Sequence Generator

To improve the model’s performance for long-tailed users, the pseudo-sequence generator (PSG) functions as a recall model, generating sequences of items aligned with user interests but not yet interacted with, in each domain. These augmented interaction records, known as pseudo-sequences, provide useful context to downstream models, even when the user’s historical behavior is sparse.

In the PSG, items from both domains are remapped to form a unified item set $V = V^X \cup V^Y$ with no duplicates. Then, based on the interaction data $\mathcal{E} = \mathcal{E}^X \cup \mathcal{E}^Y$ between the unified user set $U = U^X \cup U^Y$ and V , we build a user-item bipartite graph \mathcal{G} containing users’ interactions in both domains. We use LightGCN [7] to learn from \mathcal{E} and produce user and item embeddings: $\mathbf{E}_u \in \mathbb{R}^{|U| \times d}$ and $\mathbf{E}_v \in \mathbb{R}^{|V| \times d}$, where d is the embedding dimension. The rating matrix $\mathbf{R} \in \mathbb{R}^{M \times N}$, representing predicted users’ preferences for each item, is calculated as $\mathbf{R} = \mathbf{E}_u \cdot \mathbf{E}_v^T$. For each user, the PSG generates pseudo-sequences \tilde{S}^X and \tilde{S}^Y containing user’s original interaction sequences S^X and S^Y , along with the highest-rated items from R_u that the user has not yet engaged with. For instance, in domain X , the pseudo-sequence is defined as: $\tilde{S}^X = S^X \cup \{\tilde{v}_1, \dots, \tilde{v}_{T'}\}$, where the expanded part is the sequence of top T' items with the highest rating score in R_u , in which $\tilde{v}_i \in V^X \setminus S^X$ for all $i = 1, \dots, T'$. The pseudo-sequence, \tilde{S}^Y , for domain Y is defined similarly. The idea behind PSG is to enrich users’ limited interaction histories with lower time costs, even though the recalled items are not so accurate. LightGCN was chosen for its training and inference efficiency and its ability to leverage higher-order connectivity, for the recalls of more reliable items.

3.2 Embedding Layer

For each user, to obtain the sequential representations $\mathbf{X}^* = \{h_{S_1^X}, \dots, h_{S_T^X}\}$, $\mathbf{Y}^* = \{h_{S_1^Y}, \dots, h_{S_T^Y}\}$, $\mathbf{X}_a^* = \{h_{\tilde{S}_1^X}, \dots, h_{\tilde{S}_{T'}^X}\}$, and $\mathbf{Y}_a^* = \{h_{\tilde{S}_1^Y}, \dots, h_{\tilde{S}_{T'}^Y}\}$, we utilize embedding layers $\mathbf{E}^X \in \mathbb{R}^{|V^X| \times d}$, $\mathbf{E}^Y \in \mathbb{R}^{|V^Y| \times d}$ and the self-attention layer in SASRec [12], where d denotes the embedding dimension, T is the maximum length of the user’s interaction history, and T' is the length of pseudo-sequences generated by PSG. Next, for the above embeddings, we applied

mean-pooling over the time dimension to obtain the corresponding \mathbf{X} , \mathbf{Y} , \mathbf{X}_a , and \mathbf{Y}_a , which are in \mathbb{R}^d . Noted, when the sequence length of the interaction history is bigger than T , we only consider the most recent T actions. While the sequence length is less than T , we repeatedly add a ‘padding’ item to the left until the length is T . Moreover, we introduce learnable position embedding matrixes $\mathbf{P}_S \in \mathbb{R}^{T \times d}$ and $\mathbf{P}_A \in \mathbb{R}^{T' \times d}$ to improve the ordered information of sequence embeddings. Please note that \mathbf{X} and \mathbf{Y} are representations of the user’s behaviors, while \mathbf{X} and \mathbf{Y} denote domain names.

3.3 Inference and Generative Procedures

In the context of CDSR, we assume that user interests follow an unknown bivariate distribution $P_D(x, y)$, where the next items the user will interact with are sampled from this distribution. To learn the structured representation of user interests [2, 3], we factorize user interests into the following six d -dimension representations: \mathbf{Z}^X and \mathbf{Z}^Y , which capture the domain-specific characteristics from the user’s actual interaction history in each domain; \mathbf{Z}_a^X and \mathbf{Z}_a^Y , which learn inner-domain interests from the augmented pseudo-sequences; and cross-domain representations \mathbf{Z}_t^X (from domain X to Y) and \mathbf{Z}_t^Y (from domain Y to X), which capture the information that needs to be transferred across domains.

3.3.1 Inference Procedure. To learn the cross-domain and inner-domain representations, we employ the variational inference in variational autoencoders (VAEs), which approximates the true posterior with the approximate posterior q_ϕ . For posterior factorization, we assume that the six latent variables correspond to the aforementioned representations³ are conditionally independent given x and y . z_t^y and z_t^x represent cross-domain information, while z^x , z_a^x , z^y , and z_a^y represent domain-specific information (e.g., z^x and z_a^x being independent of y given x). Therefore, we have $q(z^x|x, y) = q(z^x|x)$, which is applicable to other domain-specific latent variables. Based

³We denote each lowercase latent variable as corresponding to its respective capitalized bold representation (e.g., z_t^y corresponds \mathbf{Z}_t^y).

on this assumption, we factorize the q_ϕ as follows:

$$\begin{aligned} q_\phi(z^x, z^y, z_t^y, z_t^x, z_a^x, z_a^y | x, y) \\ = q_{\phi_x}(z^x | x) q_{\phi_{yx}}(z_t^y | x, y) q_{\phi_{xa}}(z_a^x | x) \\ \cdot q_{\phi_y}(z^y | y) q_{\phi_{xy}}(z_t^x | x, y) q_{\phi_{ya}}(z_a^y | y). \end{aligned} \quad (5)$$

In Eq. 5, $\phi = \{\phi_x, \phi_{xa}, \phi_{yx}, \phi_{xy}, \phi_y\}$ denotes the encoder parameters. We assume that each factorized posterior follows a Gaussian distribution, with the mean and standard deviation vectors generated by different encoders. MLPs serve as domain-specific encoders to generate the mean and standard deviation vectors of the distributions q_{ϕ_x} and q_{ϕ_y} . For instance, in domain X , we have $\mu^x = \text{MLP}^\mu(X)$ and $\sigma^x = \text{MLP}^\sigma(X)$. The same encoding mechanism is applied to pseudo-sequence representations, X_a and Y_a , to generate the mean and sigmoid vectors of $q_{\phi_{xa}}$ and $q_{\phi_{ya}}$. For cross-domain posteriors $q_{\phi_{yx}}$ and $q_{\phi_{xy}}$, multi-head attention or MLPs can be used as cross-domain encoders to capture information transfers between domain X and Y . In attention-based cross-domain encoders for $q_{\phi_{yx}}$, we use the non-pooling embeddings of user behaviors, $X^* \in \mathbb{R}^{T \times d}$, as the query, and $Y^* \in \mathbb{R}^{T \times d}$ as the key and value to identify information transferring from domain Y to X . The mean vector μ_{yx} is calculated as $\mu_{yx} = \text{MLP}(\text{Mean}(\text{Attention}(X^*, Y^*, Y^*)))$, where $\text{Mean}(\cdot)$ is the mean-pooling operations on the time dimension and $\text{Attention}(\cdot)$ is the self-attention module. The standard deviation σ_{yx} is generated similarly. Alternatively, for the MLP-based cross-domain encoders, X and Y are concatenated and input into an MLP to compute the mean and standard deviation vectors. Then, the reparameterization trick is applied to generate latent variables. For z^x (the latent variable corresponding to the domain-specific representation Z^X), it is sampled as follows:

$$z^x = \mu^x + \sigma^x \odot \epsilon, \quad \epsilon \sim \mathcal{N}(0, \text{diag}(I)), \quad (6)$$

and other latent variables can be generated similarly.

3.3.2 Generative Procedure. We assume that x and y are conditionally independent given the six latent variables. Additionally, each domain is associated with only three latent variables. For instance, reconstructing X only involves the original sequence representation Z^X , the augmented sequence representation Z_a^X , and the cross-domain information Z_t^Y transferred from domain Y to X . Therefore, we have $p(x | z^x, z_t^y, z_a^x, z^y, z_t^x, z_a^y) = p(x | z^x, z_t^y, z_a^x)$, which similarly applies to domain Y . Based on this assumption, we maximize the likelihood of the joint distribution to learn the model parameters, which can be structured as:

$$\begin{aligned} p_\theta(x, y) = \int p_{\theta_x}(x | z^x, z_t^y, z_a^x) p_{\theta_y}(y | z^y, z_t^x, z_a^y) p(z^x) p(z^y) \\ \cdot p(z_a^x) p(z_a^y) p(z_t^x) p(z_t^y) dz^x dz^y dz_a^x dz_a^y dz_t^x dz_t^y. \end{aligned} \quad (7)$$

We set the prior distributions of cross-domain latent variables, $p(z_t^x)$ and $p(z_t^y)$, as standard normal distribution $\mathcal{N}(0, I)$. For domain-specific priors, we use normal distributions that vary in mean and standard deviation for different domains, reflecting the varying characteristics in different domains.

Then, based on the inference procedure in Eq. 5, we derive the Evidence Lower Bound (ELBO) of the optimization objective:

$$\begin{aligned} \log p(x, y) \geq \mathbb{E}_{q_{\phi_x} q_{\phi_{yx}} q_{\phi_{xa}}} [\log p(x | z^x, z_t^y, z_a^x)] \\ + \mathbb{E}_{q_{\phi_y} q_{\phi_{xy}} q_{\phi_{ya}}} [\log p(y | z^y, z_t^x, z_a^y)] \\ - D_{KL}[q(z^x | x) \| p(z^x)] - D_{KL}[q(z^y | y) \| p(z^y)] \\ - D_{KL}[q(z_t^y | x, y) \| p(z_t^y)] - D_{KL}[q(z_t^x | x, y) \| p(z_t^x)] \\ - D_{KL}[q(z_a^x | x) \| p(z_a^x)] - D_{KL}[q(z_a^y | y) \| p(z_a^y)]. \end{aligned} \quad (8)$$

The generative objective function includes the first two reconstruction terms, obtained by predicting the next item the user interacts with in domains X and Y . Specifically, we use MLPs as decoders to obtain the user's representation h_u from the learned latent variables in each domain. We then compute the dot product between h_u and each item representation h_{v_i} to predict user interest: $\hat{r}_{ui} = h_u \cdot h_{v_i}$. Then, we minimize the Binary Cross-Entropy (BCE) Loss between the predicted probabilities \hat{r}_{ui} and the interaction label y_{ui} to approximate the maximization of the reconstructed terms:

$$\mathcal{L}_{\text{BCE}} = - \sum_i (y_{ui} \log \hat{r}_{ui} + (1 - y_{ui}) \log(1 - \hat{r}_{ui})). \quad (9)$$

Moreover, six Kullback-Leibler (KL) divergences are also included to regularize the learned distributions with predefined priors.

However, a purely generative optimization objective does not ensure the structured representation of latent variables. Thus, in the next section, we introduce our designed regularization terms based on the theory of mutual information maximization and its corresponding tractable lower bound for optimization.

3.4 MIM Theory-induced Regularization

In the latent space, we aim to disentangle the domain-specific and cross-domain representations to extract pure intra- and inter-domain user interests. Meanwhile, we seek to extract useful information from the pseudo sequences that aligns with the true user interests while removing noise from unreliable samples recalled by the PSG. In this section, we will use domain X as an example to demonstrate how we design regularization terms. The regularizers for domain Y are obtained symmetrically and will not be repeated here.

3.4.1 Informative Regularizer. To ensure the cross-domain representation Z_t^Y encodes user interests that can be transferred from domain Y to domain X (e.g., common topics across the book and movie domains), we propose to maximize the interaction information $I(X; Y; Z_t^Y)$ between the representations of S^X and S^Y , and the cross-domain representation Z_t^Y . Using the definition of interaction information [23] in (Eq. 2 - Eq. 4), we can expand $I(X; Y; Z_t^Y)$ as:

$$I(X; Y; Z_t^Y) = I(X; Z_t^Y) - I(X; Z_t^Y | Y). \quad (10)$$

This equation also explains why maximizing interaction information encourages Z_t^Y to encode shared information. Specifically, when maximizing $I(X; Y; Z_t^Y)$, the first term in Eq. 10 is maximized, making Z_t^Y informative to X , while the second term is minimized if the information in Z_t^Y can also be inferred from Y .

3.4.2 Disentangle Regularizer. To encourage distinct intra- and inter-domain representations, we propose minimizing $I(Z^X; Z_t^Y)$, which disentangles the cross-domain representation Z_t^Y from the domain-specific information Z^X . During inference, Z_t^Y serves as

additional information to help reconstruct the user's inherent interests. For cold-start users in the domain X , all domain-specific representations are masked, and only Z_t^Y is used for reconstruction. Based on Eq. 3 and Eq. 4, we can decompose $I(Z^X, Z_t^Y)$ as follows:

$$I(Z^X; Z_t^Y) = I(Z^X; X) - I(Z^X; X|Z_t^Y) + I(Z^X; Z_t^Y|X) \quad (11)$$

Due to our disentangling assumption, $q(z^x|x) = q(z^x|x, z_t^y)$ holds. Therefore, the last term, $I(Z^X; Z_t^Y|X)$, in Eq. 12 vanishes:

$$I(Z^X; Z_t^Y|X) = H(Z^X|X) - H(Z^X|X, Z_t^Y) = H(Z^X|X) - H(Z^X|X) = 0$$

This results in the following derivation of $-I(Z^X; Z_t^Y)$, which maintains equality based on the chain rule of mutual information[5]:

$$\begin{aligned} -I(Z^X; Z_t^Y) &= -I(X; Z^X) + I(Z^X; X|Z_t^Y) \\ &= -I(X; Z^X) - I(X; Z_t^Y) + I(X; Z^X, Z_t^Y). \end{aligned} \quad (12)$$

This equation suggests that Z^X and Z_t^Y should be jointly informative to domain X (the third term), and the total amount of information in Z_t^Y and Z^X will be penalized (the first and second terms). Thus, maximizing Eq. 12 will naturally encourage Z_t^Y and Z^X to encode the distinct, non-overlapping information that can be informative to domain X .

3.4.3 Denoising Regularizer. The third regularization term we propose is to maximize the mutual information $I(Z^X; Z_a^Y)$ between representations of S^X and \tilde{S}^X , which helps denoise the pseudo-sequences generated by PSG, leaving the relevant information to Z^X and ignoring the irrelevant part.

We also noticed that when user behavior is overly sparse, it is crucial to use the rich information from the pseudo-sequence to enhance representations rather than excessively denoise, which would make the pseudo sequence representation too similar to the sparse real sequence. However, when real user behavior is abundant, it is necessary to enhance the denoising process to improve the model's ability to capture relevant and useful information from the pseudo-sequence. Therefore, we introduce a noise-adaptive weight λ_d^X , placing it in front of the denoising regularizer $I(Z^X, Z_a^Y)$. It increases as the richness of the user's interaction increases:

$$\lambda_d^X = \exp\left(\frac{aL^X}{T}\right) - b,$$

where L^X represents the length of the user's unpadded historical behavior in domain X , and T is the maximum length of S^X . a and b are balancing constants deciding the increasing speed and the minimum of the adaptive weight, which are set at 0.8 in our study.

3.4.4 Tractable Regularization Objectives. Combining the previous three regularizers (informative, disentangle, and denoising) in the domain X , we have the following maximization objectives:

$$\max I(X; Y; Z_t^Y) - I(Z^X; Z_t^Y) + I(Z^X; Z_a^Y), \quad (13)$$

which is equivalent to maximizing its derivative as follows, according to our previous inductions in Eq. 10 and Eq. 12:

$$\max I(X; Z^X, Z_t^Y) - I(X; Z^X) - I(X; Z_t^Y|Y) + I(Z^X; Z_a^Y) \quad (14)$$

Fortunately, based on the connection between the variation bound and the mutual information[25], a significant portion of our tractable regularization objective aligns with the terms in ELBO. Now, we provide the derivations of each term's tractable lower bound.

Lower Bound of $I(X; Z^X, Z_t^Y)$. This term is intractable since $q(x|z^x, z_t^y)$ involves an intractable integral. Therefore, we derive its lower bound using the generative distribution $p(x|z^x, z_t^y)$:

$$\begin{aligned} I(X; Z^X, Z_t^Y) &= \mathbb{E}_{q(z^x, z_t^y|x)p_D(x)} \left[\log \frac{q(x|z^x, z_t^y)}{p_D(x)} \right] \\ &= H(x) + \mathbb{E}_{q(z^x, z_t^y|x)p_D(x)} \left[\log p(x|z^x, z_t^y) \right] \\ &\quad + \mathbb{E}_{q(z^x, z_t^y)} \left[D_{\text{KL}}(q(z^x, z_t^y) \| p(x|z^x, z_t^y)) \right] \\ &\geq H(x) + \mathbb{E}_{q(z^x, z_t^y)p_D(x)} \left[\log p(x|z^x, z_t^y) \right] \\ &= H(x) + \mathbb{E}_{p_D(x, y)q(z^x|x)q(z_t^y|x, y)} \left[\log p(x|z^x, z_t^y) \right]. \end{aligned} \quad (15)$$

We find that maximizing Eq.15 aligns $p(x|z^x, z_t^y)$ with $q(x|z^x, z_t^y)$, serving as a reconstruction term. To avoid excessive redundancy in the overall objectives, we approximate this term in practice with $\mathbb{E}_{q_{\phi_x} q_{\phi_y} q_{\phi_{xa}}} [\log p(x|z^x, z_t^y, z_a^x)]$ from Eq. 8.

Lower Bound of $-I(X; Z^X)$. The second term in Eq. 14, $-I(X; Z^X)$, can be measured by Kullback-Leibler (KL) divergence with the approximation of posterior distributions as follows:

$$\begin{aligned} -I(X; Z^X) &= -\mathbb{E}_{p_D(x)} [D_{\text{KL}}[q(z^x|x) \| p(z^x)]] \\ &\geq -\mathbb{E}_{p_D(x)} [D_{\text{KL}}[q(z^x|x) \| p(z^x)]]. \end{aligned} \quad (16)$$

Lower Bound of $-I(X; Z_t^Y|Y)$. The lower bound of the third term in Eq. 14, $-I(X; Z_t^Y|Y)$, can be derived as follows:

$$\begin{aligned} -I(X; Z_t^Y|Y) &= -\mathbb{E}_{p_D(x, y)q(z_t^y|x, y)} \left[\log \frac{q(z_t^y|x, y)}{q(z_t^y|y)} \right] \\ &= -\mathbb{E}_{p_D(x, y)q(z_t^y|x, y)} \left[\log \left\{ \frac{q(z_t^y|x, y)}{r^y(z_t^y|y)} \times \frac{r^y(z_t^y|y)}{q(z_t^y|y)} \right\} \right] \\ &\geq -\mathbb{E}_{p_D(x, y)} [D_{\text{KL}}(q(z_t^y|x, y) \| r^y(z_t^y|y))]. \end{aligned} \quad (17)$$

Since $q(z_t^y|y)$ cannot be directly obtained within our framework, we utilize $r^y(z_t^y|y)$ to approximate it. Minimizing $-I(X; Z_t^Y|Y)$ enforces the byproduct, $r^y(z_t^y|y)$, to fit the cross-domain information transfer unit $q(z_t^y|x, y)$. This approach is beneficial in addressing cold-start users. When encountering cold-start users from domain X , the domain-specific representation in domain X becomes meaningless, thereby making the cross-domain encoders $q(z_t^y|x, y)$ ineffective. Therefore, we employ $r^y(z_t^y|y)$, which solely relies on information from domain Y , as a substitute for $q(z_t^y|x, y)$, to improve robustness for cold-start users.

Lower Bound of $I(Z^X; Z_a^Y)$. Lastly, the lower bound of the denoising regularizer in Eq.14 can be derived as follows:

$$\begin{aligned} I(Z^X; Z_a^Y) &= \mathbb{E}_{q(z^x, z_a^x|x)} \left[\log \frac{q(z^x, z_a^x|x)}{q(z^x|x)q(z_a^x|x)} \right] \\ &= \mathbb{E}_{q(z^x|x)q(z_a^x|z^x, x)} \left[\log \frac{q(z_a^x|x)}{q(z^x|x)} + \log \frac{q(z^x|z_a^x, x)}{q(z_a^x|x)} \right] \\ &= -\mathbb{E}_{q(z_a^x|z^x, x)} [D_{\text{KL}}(q(z^x|x) \| q(z_a^x|x))] + \epsilon, \end{aligned} \quad (18)$$

where ϵ is an intractable term $\mathbb{E}_{q(z_a^x, z^x|x)} \left[\log \frac{q(z^x|z_a^x, x)}{q(z_a^x|x)} \right]$, thus we optimize $I(Z_a^X, Z^X)$ by solely maximize the first term, the KL divergence in Eq. 18.

3.4.5 *Overall Optimization Objectives.* Lastly, we derive our overall objective by combining the ELBO in Eq. 8 and tractable regularization terms in each domain with a balancing weight λ_a and λ_t :

$$\begin{aligned} \max \{ & (1 + \lambda_t) \{ \mathbb{E}_{q_{\phi_x} q_{\phi_y} q_{\phi_{x_a}}} [\log p(x|z^x, z_t^y, z_a^x)] \\ & + \mathbb{E}_{q_{\phi_y} q_{\phi_{x_y}} q_{\phi_{y_a}}} [\log p(y|z^y, z_t^x, z_a^y)] \\ & - D_{KL} [q(z^x|x) \| p(z^x)] - D_{KL} [q(z^y|y) \| p(z^y)] \} \\ & - D_{KL} [q(z_t^y|x, y) \| p(z_t^y)] - D_{KL} [q(z_t^x|x, y) \| p(z_t^x)] \\ & - D_{KL} [q(z_a^x|x) \| p(z_a^x)] - D_{KL} [q(z_a^y|y) \| p(z_a^y)] \\ & - \lambda_t \{ D_{KL} [q(z_t^y|x, y) \| r^y(z_t^y|y)] + D_{KL} [q(z_t^x|x, y) \| r^x(z_t^x|x)] \} \\ & - \lambda_a \{ \lambda_a^x D_{KL} [q(z^x|x) \| q(z_a^x|x)] - \lambda_a^y D_{KL} [q(z^y|y) \| q(z_a^y|y)] \} \}. \end{aligned}$$

4 EXPERIMENTS

In this section, we conduct experiments to evaluate the performance of our IM-VAE. Experiments in this section intend to answer the following research questions (RQ):

- **RQ1:** How does IM-VAE perform compared to other baseline methods in the CDSR task across different user types, including long-tailed and cold-start users?
- **RQ2:** How do the different modules of IM-VAE contribute to the performance improvement of our method?
- **RQ3:** When encountering varying user-item interaction density and different numbers of overlapping users, can IM-VAE consistently achieve remarkable performance?
- **RQ4:** How do different hyperparameter settings affect the performance of our method?

4.1 Datasets

Following previous works[3, 4, 36, 37], we conducted offline experiments on the Amazon dataset⁴ that includes 24 distinct item domains. We selected 3 domain pairs for our experiments, across 6 scenes, “Game-Video”, “Cloth-Sport”, and “Phone-Elec”, with their statistics summarized in Table 1. All behavioral sequences were collected in chronological order. To address the significant information leak issues identified in previous studies [20, 21], we split users into three groups: 80% for training, 10% for validation, and 10% for testing within each domain. To simulate various real-world recommendation scenarios, we included non-overlapping users and adjusted the overlapping ratio (\mathcal{K}_o) to control the number of overlapping users across domains. Additionally, a certain proportion of overlapping users (\mathcal{K}_{cs}) were randomly designated as cold-start users for validation and testing phases. To simulate cold-start users, we randomly remove the sequence from one domain for selected overlapping users while retaining only the last user-item interaction as the ground truth.

4.2 Experiment Setting

4.2.1 *Evaluation Protocol.* To assess the effectiveness of our approach across various user types, we retained all overlapping ($\mathcal{K}_o = 100\%$) and non-overlapping users in the training set and randomly selected $\mathcal{K}_{cs} = 20\%$ of overlapping users from the test set as cold-start users, as outlined in section 3.1. We conducted separate evaluations on long-tailed users (whose interaction sequence length is less

Table 1: Statistics on the Amazon datasets.

Dataset	$ \mathcal{U} $	$ \mathcal{V} $	$ \mathcal{E} $	#O	$ S $	Density
Game	24,929	12,314	146,639	2,171	6.23	0.048%
Video	19,347	8,746	139,236		7.66	0.082%
Phone	27,320	9,478	140,886	20,342	5.36	0.054%
Elec	107,580	40,446	758,374		8.00	0.017%
Cloth	41,454	17,939	175,552	9,721	4.50	0.024%
Sport	27,209	12,654	159,098		6.10	0.046%

#O: the number of overlapping users across domains.

than the average sequence length of the bottom 80% users), cold-start users (who have historical behavior in only one domain), and all users in the test set to compare each method’s performance on different user groups, and we used the leave-one-out technique, a widely utilized method in cross-domain sequential recommendation literature [2, 4, 21]. For an unbiased evaluation and fair comparison [14, 38], we randomly sampled 999 negative items not interacted with by the user, along with one positive item representing the ground truth interaction. These items were then used to form the candidate set for ranking tests. We employed several top-N metrics to gauge the effectiveness of models, including Normalized Discounted Cumulative Gain (NDCG@10 [10]) and Hit Rate (HR@10). Higher values in all metrics indicate better model performance.

4.2.2 *Compared Methods.* To verify the effectiveness of our model, we compare IM-VAE with the following SOTA baselines which can be divided into three branches.

Single-domain recommendation methods: Multi-VAE [16] employs a VAE-based multinomial likelihood generative model and Bayesian inference to enhance traditional linear factor methods in collaborative filtering. SVAE [26] integrates a recurrent network in the VAE-based recommendation model to capture temporal information in the user’s historical interactions. SASRec [12] is a self-attention-based sequential recommendation model balancing model parsimony and complexity. **Cross-domain sequential recommendation methods:** Pi-Net [21] generates shared user embeddings by identifying different user behaviors with the gating mechanism. DASL [15] enhances cross-domain predictions with a dual-attention mechanism. C²DSR [2] employs graphical attention encoders and contrastive learning to jointly learn user’s inner- and cross-domain preferences. **Cross-domain recommendation methods:** EMCDR [22] first utilize MLPs to capture domain-specific representations, then learn the cross-domain mapping function on information-rich overlapping users. SA-VAE [27] uses VAEs to align the latent space of the target domain with that of the source domain, exploring both rigid and soft alignment. CDRIB [4] uses the information bottleneck to extract domain-shared user/item features and mitigate cold-start problems.

4.2.3 *Parameters Settings.* To ensure equitable evaluation, we standardize the hyperparameters across all approaches. Specifically, we set the embedding dimension d to 128 and the batch size to 512 for all methods. The learning rate is selected from a predetermined set of values $\{3 \times 10^{-4}, 4 \times 10^{-4}, \dots, 8 \times 10^{-4}\}$, and the Adam is set as optimizer. The training epoch is fixed at 100 to obtain optimal

⁴We utilized the Amazon 14 version available at http://jmcauley.ucsd.edu/data/amazon/index_2014.html

performance. The comparison baselines employ other hyperparameters as reported in their paper or official code implementations. For training the PSG module in IM-VAE, we set all hyperparameters to the default values as specified in LightGCN’s code implementation⁵. 20% of the training set is split as validation data to facilitate the training of PSG. The model is then trained for 1000 epochs, and the best checkpoint is used for recalling pseudo-sequences. We set the maximum length of the user’s historical behaviors T to 20 for all methods, and the maximum length of pseudo-sequences T' to 40 in our method, IM-VAE. In the inference process, the number of attention heads in the cross-domain information encoders is set to 4, and all MLP-based encoders and decoders share a hidden dimension of {32, 64, 32}. The hyperparameters λ_t and λ_a are selected from a pre-determined set of values $\{5 \times 10^{-4}, 1 \times 10^{-3}, 2 \times 10^{-3}, \dots, 5 \times 10^{-3}\}$. Each approach is run 5 times under different random seeds, and the optimal model is selected based on the highest normalized discounted cumulative gain (NDCG@10) performance on the validation set under grid searching.

4.3 Comparison Results (RQ1)

In this section, we compare the performance of IM-VAE with state-of-the-art baselines in SDR, CDSR, and CDR across three real-world datasets and six different scenes. The results are shown in Table 2. The baselines are organized according to the types of models.

Through extensive experiments, we found that IM-VAE consistently outperforms previous methods across long-tailed, cold-start, and all users. The reported best-performing models are significant w.r.t. the second best performing with p-value ≤ 0.05 . What’s more, while the improvements of the baseline methods vary across different datasets and on different types of users (e.g. referring to the underlined results), our method consistently achieves significant improvements across all datasets and users. From the experiment results, our findings are summarized as follows:

SDR V.S. CDR/CDSR. In most cases, CDR/CDSR methods outperform SDR due to the captures of cross-domain interests. This indicates the importance of utilizing rich cross-domain information to support the model’s understanding of user interests when data is sparse. Unexpectedly, SDR models like SVAE and SASRec seldom perform better than CDR/CDSR methods on cold-start users. This may be due to too few overlapping users to learn adequate cross-domain interests in the "Game" and "Cloth" domains.

For long-tailed users. Moreover, we found that long-tailed users are highly challenging for all methods. The improvements achieved by other baselines for this user group are relatively limited. This indicates that the richness of interaction history, or data density, significantly impacts model performance. Our method outperforms the second-best model with improvements ranging from 0.43% to 5.00%, because it enriches the user’s sparse interaction history with pseudo-sequences and denoises to filter out informative information as supplements, thereby enhancing model performance for long-tailed users. Notably, we believe that using other real auxiliary behaviors (e.g., views, clicks) instead of pseudo-sequences could further improve model performance for long-tailed users.

For cold-start users. Finally, IM-VAE shows significant improvement over the second-best model for cold-start users, ranging from

1.17% to 15.20%, because the designed $r^x(z_t^y|y)$ and $r^y(z_t^x|x)$ enable the cross-domain representations learning for both overlapping and non-overlapping users, addressing the previous models’ excessive reliance on overlapping users. Additionally, we implemented informative and disentangle regularizers to extract distinct cross-domain interests without domain-specific noises, further enhancing the model’s inference performance for cold-start users.

4.4 Ablation Study (RQ2)

In this section, we assess the importance of each module by examining their impact on performance. First, we remove the PSG module and replace the pseudo-sequence with a randomly generated sequence of equal length. Additionally, due to the overlapping optimization objectives of the informative and disentangle regularizers, we combined them into a single module, denoted as IF-R & DS-R, and analyzed the model’s performance after removing them from the loss. Lastly, we removed the denoising regularizer, denoted as DN-R, to evaluate its impact. The experimental results are shown in Table 3. We observed that removing any single module results in a decrease in model performance across all metrics compared to the original IM-VAE. Our findings can be summarized as follows:

- Replacing pseudo-sequences generated by PSG with random sequence results in a performance decline across all types of users, indicating the augmenting user’s behaviors with a not-so-accurate recall model still improves the understanding of user’s interests.
- Removing the informative regularizer and disentangle regularizer (IF-R & DS-R) also leads to a decline in performance across all types of users, indicating that the structured representation plays a significant role in the model’s better understanding of users’ latent interests. However, the removal of IF-R & DS-R has the greatest impact on cold-start users. This suggests that expanding training to non-overlapping users and disentangling domain-specific information, is crucial for cold-start users.
- Removing DN-R also leads to a decline in performance across all types of users, indicating that treating pseudo-sequences and real interaction sequences indiscriminately is problematic. It highlights the importance of using DS-R to capture reliable and informative information from pseudo-sequences while eliminating unreliable noise. We also found that removing DN-R has the greatest impact on the model’s performance for long-tailed users. This suggests that when users’ inner-domain interaction records are insufficient, using reliable pseudo-sequences to supplement and enhance the information is an effective approach.

4.5 Model Analysis (RQ3)

4.5.1 Discussion of Behavior Sparsity. To verify the superior performance of IM-VAE in CDSR scenarios with varying data densities, we conduct further studies by varying the data density D_s in {25%, 50%, 75% 100%}. As the density decreases, the actual user-item interaction records in the training and testing sets are down-sampled, thereby testing the robustness of our IM-VAE’s and the second-best SA-VAE’s performance on much sparser datasets. We re-run the experiments of two comparing methods on the 'Cloth-Sport' dataset with other settings same as in Sections 3.2.1 and 3.2.3. The experimental results of our model (IM-VAE) compared to the second-best baseline (SAVAE) are presented in Table 4. All experiments were

⁵<https://github.com/gusye1234/LightGCN-PyTorch>

Table 2: Experimental Results (%) across different types of users, including long-tailed(tailed) users, cold-start users, and all users, on Game-Video, Phone-Elec, and Cloth-Sport CDSR datasets, respectively.

Datasets	User Types	Metric	SDR			CDR-sequential			CDR			Ours	↑(%)
			Multi-VAE [16]	SVAE [26]	SASRec [12]	DASL [15]	PiNet [21]	C ² DSR [2]	EMCDR [22]	SA-VAE [27]	CDRIB [4]	IM-VAE	
Game	Tailed	NDCG	5.08±0.14	5.17±0.08	5.12±0.19	4.64±0.25	4.64±0.25	5.04±0.08	5.31±0.21	<u>5.31±0.15</u>	5.23±0.14	5.51±0.12	3.77
		HR	9.48±0.38	9.46±0.14	9.39±0.34	8.45±0.38	8.45±0.38	9.34±0.17	9.67±0.3	<u>9.95±0.39</u>	9.68±0.35	10.09±0.18	1.41
	Cold-start	NDCG	9.13±0.64	<u>9.97±1.37</u>	8.61±1.92	7.46±0.93	7.46±0.93	9.18±1.57	8.97±1.49	9.69±1.09	7.72±1.63	10.92±0.7	9.53
		HR	20.0±3.95	19.15±1.9	16.6±2.48	15.32±1.59	15.32±1.59	16.17±2.89	17.87±1.7	<u>19.57±1.59</u>	15.74±2.89	22.55±2.17	15.20
	All	NDCG	5.39±0.15	5.40±0.09	<u>5.57±0.1</u>	4.82±0.21	4.82±0.21	5.53±0.11	5.48±0.15	<u>5.51±0.09</u>	5.30±0.05	5.79±0.12	4.01
		HR	9.95±0.30	9.94±0.18	10.20±0.30	8.87±0.22	8.87±0.22	10.28±0.23	10.16±0.20	<u>10.32±0.04</u>	9.92±0.19	10.61±0.15	2.77
Video	Tailed	NDCG	6.79±0.11	6.86±0.1	6.82±0.18	6.32±0.18	6.32±0.18	6.75±0.2	6.84±0.15	6.88±0.1	<u>7.05±0.08</u>	7.08±0.14	0.43
		HR	12.43±0.19	12.5±0.18	12.26±0.39	11.46±0.36	11.46±0.36	12.34±0.35	12.54±0.36	<u>12.57±0.25</u>	<u>12.68±0.22</u>	12.95±0.26	2.13
	Cold-start	NDCG	7.4±2.13	8.19±1.5	7.93±1.39	8.1±3.21	8.1±3.21	<u>8.73±1.17</u>	8.12±1.55	8.54±2.13	8.26±1.71	9.62±1.58	10.10
		HR	18.67±2.67	21.78±3.27	20.0±2.43	17.78±4.66	17.78±4.66	<u>21.78±2.59</u>	19.11±1.78	19.11±3.61	20.44±2.18	22.67±2.18	4.09
	All	NDCG	6.49±0.09	6.59±0.1	6.5±0.11	5.87±0.15	5.87±0.15	6.46±0.19	6.6±0.17	6.58±0.16	<u>6.67±0.11</u>	6.79±0.09	1.80
		HR	12.1±0.16	12.18±0.14	11.97±0.31	10.92±0.22	10.92±0.22	12.14±0.25	12.24±0.18	12.32±0.29	<u>12.33±0.16</u>	12.67±0.18	2.76
Phone	Tailed	NDCG	3.58±0.13	3.51±0.11	3.41±0.13	<u>4.10±0.15</u>	3.68±0.17	3.81±0.17	4.01±0.14	4.06±0.31	4.01±0.23	4.23±0.21	3.17
		HR	6.90±0.34	6.74±0.20	6.58±0.32	<u>8.06±0.27</u>	7.17±0.20	7.47±0.39	7.78±0.39	7.96±0.61	7.92±0.38	8.17±0.27	1.36
	Cold-start	NDCG	3.16±0.19	3.15±0.30	2.97±0.38	<u>3.63±0.25</u>	3.51±0.38	3.73±0.37	3.80±0.33	3.83±0.48	<u>4.00±0.35</u>	4.39±0.21	9.75
		HR	6.26±0.39	6.11±0.42	6.03±0.45	7.40±0.39	7.18±0.51	7.18±0.74	7.56±0.56	<u>7.94±0.85</u>	7.56±0.51	8.63±0.19	8.69
	All	NDCG	3.98±0.19	3.89±0.06	3.88±0.14	4.40±0.17	4.13±0.14	4.36±0.21	<u>4.52±0.15</u>	4.49±0.29	4.46±0.19	5.79±0.29	3.23
		HR	7.59±0.39	7.33±0.14	7.36±0.27	8.54±0.32	7.77±0.34	8.30±0.38	8.68±0.22	8.54±0.50	8.66±0.29	10.61±0.22	2.35
Elec	Tailed	NDCG	6.96±0.23	6.74±0.25	6.78±0.29	7.63±0.19	7.09±0.24	7.78±0.13	7.64±0.10	7.60±0.30	<u>7.77±0.11</u>	8.00±0.10	2.96
		HR	11.65±0.48	11.39±0.47	11.49±0.53	<u>12.83±0.41</u>	11.66±0.56	13.05±0.28	12.45±0.25	12.56±0.39	12.66±0.28	13.49±0.19	5.14
	Cold-start	NDCG	9.35±0.33	9.22±0.19	9.16±0.19	9.73±0.65	9.59±0.35	9.85±0.30	<u>9.90±0.25</u>	9.76±0.48	9.73±0.40	10.26±0.42	3.64
		HR	14.71±0.49	14.76±0.60	14.94±0.51	15.76±1.24	15.00±1.00	15.94±0.43	15.24±0.60	15.35±0.90	15.53±0.34	17.12±0.39	7.40
	All	NDCG	8.20±0.22	8.06±0.27	8.08±0.34	8.58±0.16	7.84±0.08	9.00±0.12	8.95±0.13	8.84±0.19	<u>9.04±0.04</u>	9.33±0.09	3.22
		HR	13.08±0.43	12.81±0.45	12.86±0.59	13.60±0.50	12.31±0.19	<u>14.46±0.31</u>	14.03±0.21	13.96±0.26	14.08±0.26	15.28±0.26	5.64
Cloth	Tailed	NDCG	2.31±0.08	2.07±0.16	2.09±0.20	2.28±0.17	2.11±0.17	2.29±0.09	2.24±0.09	<u>2.40±0.14</u>	2.27±0.10	2.52±0.07	5.00
		HR	4.15±0.12	3.99±0.34	3.99±0.31	<u>4.46±0.24</u>	4.15±0.36	4.38±0.32	4.27±0.20	4.43±0.22	4.21±0.21	4.73±0.16	6.05
	Cold-start	NDCG	3.23±0.29	<u>3.41±0.35</u>	2.86±0.50	3.28±0.18	3.04±0.66	3.08±0.65	3.03±0.29	3.25±0.24	3.00±0.39	3.45±0.35	1.17
		HR	6.08±0.38	<u>6.39±0.43</u>	5.64±0.86	6.27±0.40	5.58±1.24	5.96±0.95	5.96±0.56	5.89±0.46	5.52±0.58	6.77±0.51	5.95
	All	NDCG	2.20±0.10	2.18±0.1	2.11±0.15	2.43±0.09	2.18±0.10	2.40±0.07	2.37±0.07	<u>2.52±0.10</u>	2.39±0.06	2.59±0.11	2.78
		HR	4.25±0.12	4.28±0.28	4.15±0.30	<u>4.82±0.11</u>	4.24±0.18	4.63±0.18	4.65±0.19	4.81±0.19	4.56±0.09	5.00±0.17	3.73
Sport	Tailed	NDCG	3.02±0.14	2.90±0.16	2.80±0.21	<u>3.31±0.36</u>	2.96±0.15	3.06±0.15	3.23±0.07	3.29±0.15	3.12±0.11	3.36±0.10	1.51
		HR	6.06±0.50	5.76±0.34	5.72±0.22	6.29±0.57	5.89±0.25	6.03±0.22	6.20±0.31	<u>6.31±0.42</u>	5.81±0.10	6.66±0.17	5.55
	Cold-start	NDCG	4.33±0.49	4.19±0.24	3.92±0.40	4.48±0.42	4.24±0.31	4.65±0.53	4.93±0.18	<u>5.05±0.29</u>	4.95±0.25	5.43±0.29	7.52
		HR	8.89±0.66	8.62±0.73	7.88±0.62	8.15±0.94	8.28±0.27	9.36±0.54	9.49±0.49	<u>9.63±0.73</u>	9.09±0.43	10.30±0.46	6.96
	All	NDCG	3.79±0.07	3.89±0.15	3.70±0.18	3.93±0.14	3.68±0.08	4.13±0.17	4.21±0.13	<u>4.31±0.13</u>	4.27±0.09	4.40±0.10	2.20
		HR	7.23±0.27	7.27±0.29	7.00±0.17	7.45±0.32	6.90±0.33	7.84±0.33	7.90±0.22	<u>8.06±0.26</u>	7.88±0.33	8.53±0.14	5.80

Table 3: Experiment results (%) of the ablation study on Cloth-Sport dataset.

Domain	User Types	Metric	Model Variants			IM-VAE
			w/o PSG	w/o IF-R&DS-R	w/o DN-R	
Cloth	Tailed	NDCG	2.41±0.14	2.38±0.09*	2.39±0.14	2.52 ±0.07
		HR	4.59±0.12	4.49±0.21	4.45±0.21*	4.73 ±0.16
	Cold-Start	NDCG	3.21±0.22*	3.23±0.12	3.30±0.17	3.45 ±0.35
		HR	6.21±0.23*	6.27±0.34	6.46±0.58	6.77 ±0.51
	All	NDCG	2.54±0.12	2.54±0.11*	2.54±0.12	2.59 ±0.11
		HR	4.92±0.20	4.84±0.26*	4.89±0.23	5.00 ±0.17
Sport	Tailed	NDCG	3.35±0.12	3.28±0.11	3.27±0.07*	3.36 ±0.10
		HR	6.51±0.24	6.39±0.16	6.33±0.18*	6.66 ±0.17
	Cold-Start	NDCG	5.26±0.26	5.18±0.30*	5.19±0.28	5.43 ±0.29
		HR	10.24±0.46	9.90±0.34*	10.10±0.43	10.30 ±0.46
	All	NDCG	4.36±0.05	4.31±0.16*	4.32±0.15	4.40 ±0.10
		HR	8.44±0.14	8.41±0.25*	8.44±0.24	8.53 ±0.14

* indicates the model variant with the lowest evaluation metric on the current user group.

Table 4: Experiment results (%) on Cloth-Sport datasets with different density (D_s).

Domain	User	Metric	$D_s = 25\%$		$D_s = 50\%$		$D_s = 75\%$		$D_s = 100\%$	
			SA-VAE	IM-VAE	SA-VAE	IM-VAE	SA-VAE	IM-VAE	SA-VAE	IM-VAE
Cloth	Tailed	NDCG	1.39	<u>1.51</u>	1.40	<u>1.53</u>	1.40	<u>1.46</u>	2.40	<u>2.52</u>
		HR	2.75	<u>2.96</u>	2.69	<u>2.88</u>	2.85	<u>2.95</u>	4.43	<u>4.73</u>
	Cold-Start	NDCG	0.84	<u>0.85</u>	0.9	<u>1.12</u>	1.41	<u>1.72</u>	3.25	<u>3.45</u>
		HR	1.94	<u>1.82</u>	2.26	<u>2.26</u>	2.82	<u>3.32</u>	5.89	<u>6.77</u>
	All	NDCG	1.38	<u>1.49</u>	1.39	<u>1.53</u>	1.42	<u>1.57</u>	2.52	<u>2.59</u>
		HR	2.74	<u>2.95</u>	2.71	<u>2.92</u>	2.95	<u>3.27</u>	4.81	<u>5.00</u>
Sport	Tailed	NDCG	2.35	<u>2.53</u>	2.47	<u>2.72</u>	2.8	<u>3.26</u>	3.29	<u>3.36</u>
		HR	4.27	<u>4.62</u>	4.41	<u>5.09</u>	4.86	<u>5.66</u>	6.31	<u>6.66</u>
	Cold-Start	NDCG	0.71	<u>0.76</u>	0.99	<u>1.06</u>	1.88	<u>2.14</u>	5.05	<u>5.43</u>
		HR	1.62	<u>1.48</u>	2.02	<u>2.02</u>	3.57	<u>3.84</u>	9.63	<u>10.30</u>
	All	NDCG	2.49	<u>2.70</u>	3.03	<u>3.28</u>	3.18	<u>3.70</u>	4.31	<u>4.40</u>
		HR	4.46	<u>4.84</u>	5.47	<u>6.16</u>	5.62	<u>6.60</u>	8.06	<u>8.53</u>

SA-VAE outperforms IM-VAE in only one metric (underlined), likely due to the high variance on cold-start users in extremely sparse conditions ($D_s = 25\%$).

conducted five times under different random seeds, and the average values were reported.

As expected, the overall performance of both models decreases with decreasing data density, as sparser data makes representation learning and knowledge transfer more challenging. The comparing method, SA-VAE, shows a significant decline in performance as density decreases. This is because SA-VAE significantly relies

Table 5: Experiment results (%) on Cloth-Sport dataset with the varying overlapping ratio (\mathcal{K}_o).

Domain	User	Metric	$\mathcal{K}_o = 25\%$		$\mathcal{K}_o = 50\%$		$\mathcal{K}_o = 75\%$		$\mathcal{K}_o = 100\%$	
			SA-VAE	IM-VAE	SA-VAE	IM-VAE	SA-VAE	IM-VAE	SA-VAE	IM-VAE
Cloth	Tailed	NDCG	0.93	1.32	1.69	1.87	2.25	2.30	2.40	2.52
		HR	2.02	2.72	3.24	3.70	4.26	4.50	4.43	4.73
	Cold-Start	NDCG	0.95	1.62	2.19	2.52	3.26	3.27	3.25	3.45
		HR	2.07	3.39	4.83	5.20	6.27	6.21	5.89	6.77
	All	NDCG	0.92	1.31	1.71	1.93	2.29	2.42	2.52	2.59
		HR	1.94	2.71	3.43	3.97	4.40	4.75	4.81	5.00
Sport	Tailed	NDCG	1.15	1.92	2.31	2.77	3.07	3.36	3.29	3.36
		HR	2.48	4.06	4.59	5.60	5.82	6.62	6.31	6.66
	Cold-Start	NDCG	1.58	2.93	3.57	4.48	4.80	5.27	5.05	5.43
		HR	3.37	6.13	6.80	8.82	9.29	10.51	9.63	10.30
	All	NDCG	1.45	2.65	3.08	3.85	4.03	4.28	4.31	4.40
		HR	2.97	5.35	5.88	7.53	7.65	8.22	8.06	8.53

on rich user interactions within each domain to learn good inner-domain and cross-domain user interest representations. In contrast, our model generally achieves better recommendation results than SA-VAE as the dataset becomes increasingly sparse, with less performance degradation. We believe this is mainly due to our PSG module generating pseudo-sequences and the de-noise regularizer, serves as a supplement to the sparse interaction data, allowing IM-VAE to perform better than SA-VAE in sparse data conditions.

4.5.2 Discussion of Overlapping Ratio. We also designed experiments to test our model’s performance with fewer cross-domain overlapping users. In this experiment, we randomly downsampled the proportion of overlapping users (\mathcal{K}_o) in the training set, keeping the test set unchanged. We then reran the experiments to compare our model with the second-best model, SA-VAE, at \mathcal{K}_o values of 25%, 50%, 75%, 100%. This experiment aims to simulate real-world recommendation environments, requiring the model to maintain stable recommendation performance despite facing a few overlapping users in training data. The results are shown in Table 5.

We found that as the number of overlapping users decreases, the performance of both SA-VAE and our model declines across all users, due to the increased difficulty in capturing cross-domain signals. However, our model outperforms SA-VAE at every \mathcal{K}_o level. This is because our model does not rely solely on overlapping users for learning. Although capturing cross-domain information becomes harder, our denoise pseudo-sequence can still effectively capture intra-domain interests, supporting the model’s recommendation performance within domains. Additionally, the informative and disentangle information regularizer’s encoders r^x and r^y allow training on non-overlapping users for cross-domain signals based on behaviors in one domain. Consequently, our model performs better in this experiment setting compared to SA-VAE, which relies on overlapping users to learn the mapping function for cross-domain latent spaces.

4.6 Parameter Sensitivity (RQ4)

In this section, we investigate the parameter sensitivity of the sequence length T and the harmonic factors λ_a and λ_t .

In Figures 3 (a) and (b), we show the impact of sequence length T varying in the set $\{10, 15, 20, 25, 30\}$ on model performance (HR@10) for different types of users in the Cloth and Sport domains. As can be seen, the model generally performs best when $T = 20$. When increasing T from 10 to 20, the performance improves due to the richer historical interest information. However, if T is larger than

20, the performance decreases because padding items cause the model to ignore important information from the true interactions.

In Figures 3 (c) and (d), we show the impact of varying λ_a in the set $\{0.001, 0.002, \dots, 0.010\}$ on the model performance for different users in the Cloth and Sport domains, with λ_t fixed at 0.001. Similar to VAE-based work [4], λ_a significantly influences the model’s performance, exhibiting different degrees of nonlinear effects on various types of users. However, the model generally performs best for all user types when λ_a is around 0.004 and 0.005, indicating that this setting allows the denoising module to be effective without depressing the classification loss. Similarly, when fixing λ_a to 0.005, the impact of λ_t mirrors that of λ_a , shown in Figures 3 (e) and (f), with superior results achieved when λ_t is set to 0.001 or 0.005.

5 RELATED WORK

In this section, we briefly review the previous related works from aspects both in CDSR and VAE-based methods.

Cross-Domain Sequential Recommendation (CDSR) [21, 30, 37] aims to improve sequential recommendation (SR) performance by utilizing user behavior sequences from multiple related domains. Pi-Net[21] and PSJNet [30] design gating mechanism to learn and transfer cross-domain information on overlapping users. The attentive learning-based model DASL [15] uses dual attentive learning to transfer the user’s latent interests bidirectionally across two domains. Similarly, DA-GCN[6] and MIFN[20] build user-item bipartite graphs to facilitate cross-domain information transferring on overlapping users. Moreover, C²DSR [2] employs graph neural networks [7, 19, 33, 34] and sequential attentive encoder to simultaneously learn the inter-domain and inner-domain collaborative signals and utilize contrastive learning to align single-domain and cross-domain user representations. However, these methods rely heavily on data from overlapping users, who constitute only a small fraction of the user base in real-world scenarios, thereby, they usually perform poorly in real-world recommendation systems due to inadequate representation of long-tailed and cold-start users.

VAE-based Recommendation [13, 16] have become prominent for their strong probabilistic foundations in exploring the complexities of user-item interactions within latent spaces. SA-VAE [27] pre-trains a VAE on the source domain and aligns latent variables between source and target domain VAEs. DisenCDR [3] uses mutual information maximization to disentangle domain-specific information. Both methods rely on user overlap and perform poorly for non-overlapping users. To address this, VDEA [18] uses VAEs with embedding alignment to enhance performance for non-overlapping users, while CDRIB [4] employs a variational information bottleneck to model domain-shared and inner-domain information for cold-start users. However, CDRIB is limited to cold-start users and compresses information-rich inner-domain data, affecting performance for overlapping users.

6 CONCLUSION

In this paper, we propose a novel CDSR model, IM-VAE, which innovatively addresses long-tailed and cold-start users in real-world recommendation environments. Our model introduces MIM-theory-induced informative, disentangle, and denoising regularizers. These regularizers enable the learning of distinct inner- and cross-domain

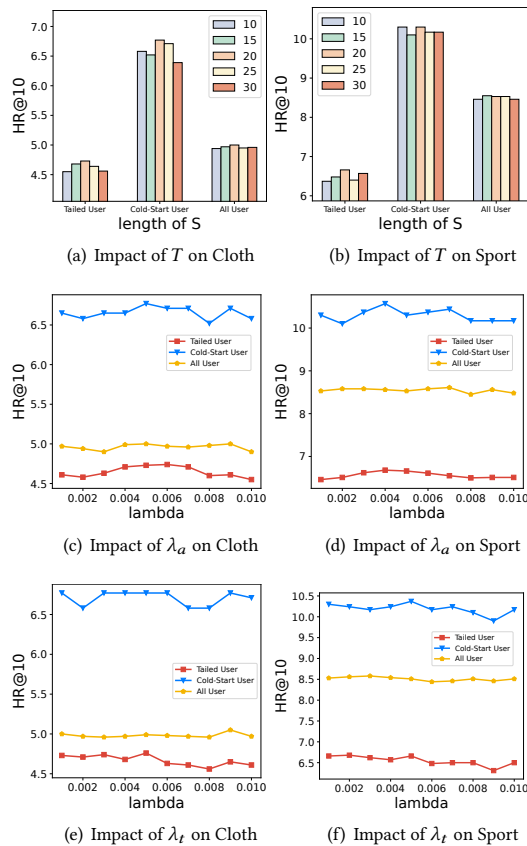


Figure 3: Parts (a) and (b) illustrate the effect of sequence length T on the model's performance (HR@10) within the "Cloth" and "Sport" domains respectively. Similarly, parts (c) and (d) demonstrate the impact of λ_a , while parts (e) and (f) highlight the effect of λ_t on the model's performance (HR@10) across the same domains.

interests and extracting relevant information from pseudo-sequences to enrich users' sparse interaction records, to improve the model's effectiveness in real-world CDSR scenarios.

REFERENCES

- [1] Mohamed Ishmael Belghazi, Aristide Baratin, Sai Rajeshwar, Sherjil Ozair, Yoshua Bengio, Aaron Courville, and Devon Hjelm. 2018. Mutual information neural estimation. In *International conference on machine learning*. PMLR, 531–540.
- [2] Jiangxia Cao, Xin Cong, Jiawei Sheng, Tingwen Liu, and Bin Wang. 2022. Contrastive Cross-Domain Sequential Recommendation. In *Proceedings of the 31st ACM International Conference on Information & Knowledge Management*. 138–147.
- [3] Jiangxia Cao, Xixun Lin, Xin Cong, Jing Ya, Tingwen Liu, and Bin Wang. 2022. Disencdr: Learning disentangled representations for cross-domain recommendation. In *Proceedings of the 45th International ACM SIGIR Conference on Research and Development in Information Retrieval*. 267–277.
- [4] Jiangxia Cao, Jiawei Sheng, Xin Cong, Tingwen Liu, and Bin Wang. 2022. Cross-domain recommendation to cold-start users via variational information bottleneck. In *2022 IEEE 38th International Conference on Data Engineering (ICDE)*. IEEE, 2209–2223.
- [5] Thomas M Cover. 1999. *Elements of information theory*. John Wiley & Sons.
- [6] Lei Guo, Li Tang, Tong Chen, Lei Zhu, Quoc Viet Hung Nguyen, and Hongzhi Yin. 2021. DA-GCN: A domain-aware attentive graph convolution network for shared-account cross-domain sequential recommendation. *arXiv preprint arXiv:2105.03300* (2021).
- [7] Xiangnan He, Kuan Deng, Xiang Wang, Yan Li, Yongdong Zhang, and Meng Wang. 2020. Lightgcn: Simplifying and powering graph convolution network for recommendation. In *Proceedings of the 43rd International ACM SIGIR conference on research and development in Information Retrieval*. 639–648.
- [8] Balázs Hidasi, Alexandros Karatzoglou, Linas Baltrunas, and Domonkos Tikk. 2015. Session-based recommendations with recurrent neural networks. *arXiv preprint arXiv:1511.06939* (2015).
- [9] R Devon Hjelm, Alex Fedorov, Samuel Lavoie-Marchildon, Karan Grewal, Phil Bachman, Adam Trischler, and Yoshua Bengio. 2018. Learning deep representations by mutual information estimation and maximization. *arXiv preprint arXiv:1808.06670* (2018).
- [10] Kalervo Järvelin and Jaana Kekäläinen. 2002. Cumulated gain-based evaluation of IR techniques. *ACM Transactions on Information Systems (TOIS)* 20, 4 (2002), 422–446.
- [11] SeongKu Kang, Junyoung Hwang, Dongha Lee, and Hwanjo Yu. 2019. Semi-supervised learning for cross-domain recommendation to cold-start users. In *Proceedings of the 28th ACM international conference on information and knowledge management*. 1563–1572.
- [12] Wang-Cheng Kang and Julian McAuley. 2018. Self-attentive sequential recommendation. In *2018 IEEE international conference on data mining (ICDM)*. IEEE, 197–206.
- [13] Diederik P Kingma and Max Welling. 2013. Auto-encoding variational bayes. *arXiv preprint arXiv:1312.6114* (2013).
- [14] Walid Krichene and Steffen Rendle. 2020. On sampled metrics for item recommendation. In *Proceedings of the 26th ACM SIGKDD international conference on knowledge discovery & data mining*. 1748–1757.
- [15] Pan Li, Zhichao Jiang, Maofei Que, Yao Hu, and Alexander Tuzhilin. 2021. Dual attentive sequential learning for cross-domain click-through rate prediction. In *Proceedings of the 27th ACM SIGKDD conference on knowledge discovery & data mining*. 3172–3180.
- [16] Dawen Liang, Rahul G Krishnan, Matthew D Hoffman, and Tony Jebara. 2018. Variational autoencoders for collaborative filtering. In *Proceedings of the 2018 world wide web conference*. 689–698.
- [17] Xixun Lin, Jia Wu, Chuan Zhou, Shirui Pan, Yanan Cao, and Bin Wang. 2021. Task-adaptive neural process for user cold-start recommendation. In *Proceedings of the Web Conference 2021*. 1306–1316.
- [18] Weiming Liu, Xiaolin Zheng, Jiajie Su, Mengling Hu, Yanchao Tan, and Chaochao Chen. 2022. Exploiting Variational Domain-Invariant User Embedding for Partially Overlapped Cross Domain Recommendation. In *Proceedings of the 45th International ACM SIGIR Conference on Research and Development in Information Retrieval*. 312–321.
- [19] Chen Ma, Liheng Ma, Yingxue Zhang, Jianing Sun, Xue Liu, and Mark Coates. 2020. Memory augmented graph neural networks for sequential recommendation. In *Proceedings of the AAAI conference on artificial intelligence*, Vol. 34. 5045–5052.
- [20] Muyang Ma, Pengjie Ren, Zhumin Chen, Zhaochun Ren, Lifan Zhao, Peiyu Liu, Jun Ma, and Maarten de Rijke. 2022. Mixed information flow for cross-domain sequential recommendations. *ACM Transactions on Knowledge Discovery from Data (TKDD)* 16, 4 (2022), 1–32.
- [21] Muyang Ma, Pengjie Ren, Yujie Lin, Zhumin Chen, Jun Ma, and Maarten de Rijke. 2019. π -net: A parallel information-sharing network for shared-account cross-domain sequential recommendations. In *Proceedings of the 42nd international ACM SIGIR conference on research and development in information retrieval*. 685–694.
- [22] Tong Man, Huawei Shen, Xiaolong Jin, and Xueqi Cheng. 2017. Cross-domain recommendation: An embedding and mapping approach. In *IJCAI*, Vol. 17. 2464–2470.
- [23] William McGill. 1954. Multivariate information transmission. *Transactions of the IRE Professional Group on Information Theory* 4, 4 (1954), 93–111.
- [24] Liam Paninski. 2003. Estimation of entropy and mutual information. *Neural computation* 15, 6 (2003), 1191–1253.
- [25] Ben Poole, Sherjil Ozair, Aaron Van Den Oord, Alex Alemi, and George Tucker. 2019. On variational bounds of mutual information. In *International Conference on Machine Learning*. PMLR, 5171–5180.
- [26] Naveen Sachdeva, Giuseppe Manco, Ettore Ritacco, and Vikram Pudi. 2019. Sequential variational autoencoders for collaborative filtering. In *Proceedings of the twelfth ACM international conference on web search and data mining*. 600–608.
- [27] Aghiles Salah, Thanh Binh Tran, and Hady Lauw. 2021. Towards source-aligned variational models for cross-domain recommendation. In *Proceedings of the 15th ACM Conference on Recommender Systems*. 176–186.
- [28] Jiarui Shi and Quanmin Wang. 2019. Cross-domain variational autoencoder for recommender systems. In *2019 IEEE 11th International Conference on Advanced Infocomm Technology (ICAIT)*. IEEE, 67–72.
- [29] Fei Sun, Jun Liu, Jian Wu, Changhua Pei, Xiao Lin, Wenwu Ou, and Peng Jiang. 2019. BERT4Rec: Sequential recommendation with bidirectional encoder representations from transformer. In *Proceedings of the 28th ACM international conference on information and knowledge management*. 1441–1450.
- [30] Wenchao Sun, Muyang Ma, Pengjie Ren, Yujie Lin, Zhumin Chen, Zhaochun Ren, Jun Ma, and Maarten De Rijke. 2021. Parallel split-join networks for shared account cross-domain sequential recommendations. *IEEE Transactions on Knowledge and Data Engineering* 35, 4 (2021), 4106–4123.

- [31] Jiayi Tang and Ke Wang. 2018. Personalized top-n sequential recommendation via convolutional sequence embedding. In *Proceedings of the eleventh ACM international conference on web search and data mining*. 565–573.
- [32] Jianling Wang, Kaize Ding, Liangjie Hong, Huan Liu, and James Caverlee. 2020. Next-item recommendation with sequential hypergraphs. In *Proceedings of the 43rd international ACM SIGIR conference on research and development in information retrieval*. 1101–1110.
- [33] Runzhong Wang, Junchi Yan, and Xiaokang Yang. 2020. Combinatorial learning of robust deep graph matching: an embedding based approach. *IEEE Transactions on Pattern Analysis and Machine Intelligence* 45, 6 (2020), 6984–7000.
- [34] Xiang Wang, Tinglin Huang, Dingxian Wang, Yancheng Yuan, Zhenguang Liu, Xiangnan He, and Tat-Seng Chua. 2021. Learning intents behind interactions with knowledge graph for recommendation. In *Proceedings of the web conference 2021*. 878–887.
- [35] Wujiang Xu, Shaoshuai Li, Mingming Ha, Xiaobo Guo, Qiongxiu Ma, Xiaolei Liu, Linxun Chen, and Zhenfeng Zhu. 2023. Neural Node Matching for Multi-Target Cross Domain Recommendation. *arXiv preprint arXiv:2302.05919* (2023).
- [36] Wujiang Xu, Xuying Ning, Wenfang Lin, Mingming Ha, Qiongxiu Ma, Linxun Chen, Bing Han, and Minnan Luo. 2023. Towards open-world cross-domain sequential recommendation: A model-agnostic contrastive denoising approach. *arXiv preprint arXiv:2311.04760* (2023).
- [37] Wujiang Xu, Qitian Wu, Runzhong Wang, Mingming Ha, Qiongxiu Ma, Linxun Chen, Bing Han, and Junchi Yan. 2023. Rethinking cross-domain sequential recommendation under open-world assumptions. *arXiv preprint arXiv:2311.04590* (2023).
- [38] Wayne Xin Zhao, Junhua Chen, Pengfei Wang, Qi Gu, and Ji-Rong Wen. 2020. Revisiting alternative experimental settings for evaluating top-n item recommendation algorithms. In *Proceedings of the 29th ACM International Conference on Information & Knowledge Management*. 2329–2332.
- [39] Yongchun Zhu, Kaikai Ge, Fuzhen Zhuang, Ruobing Xie, Dongbo Xi, Xu Zhang, Leyu Lin, and Qing He. 2021. Transfer-meta framework for cross-domain recommendation to cold-start users. In *Proceedings of the 44th international ACM SIGIR conference on research and development in information retrieval*. 1813–1817.